JCTC Journal of Chemical Theory and Computation

Article

pubs.acs.org/JCTC

Variational, Self-Consistent Implementation of the Perdew–Zunger Self-Interaction Correction with Complex Optimal Orbitals

Susi Lehtola*[,†,¶] and Hannes Jónsson[†,‡]

[†]COMP Centre of Excellence and Department of Applied Physics, P.O. Box 11100, FI-00076 Aalto University, Espoo, Finland

[‡]Faculty of Physical Sciences, University of Iceland, Reykjavík, Iceland

ABSTRACT: A variational, self-consistent implementation of the Perdew–Zunger self-interaction correction (PZ-SIC), based on a unified Hamiltonian and complex optimal orbitals, is presented for finite systems and atom-centered basis sets. A simplifying approximation allowing the use of real canonical orbitals is proposed. The algorithm is based on two-step self-consistent field iterations, where the updates of the canonical orbitals and the optimal orbitals are done separately. Calculations of the energy of atoms ranging from H to Ar are presented, using various generalized gradient functionals (PBE, APBE, PBEsol) and a meta-generalized gradient functional (TPSS). While the energy of atoms is poorly described by PBEsol, which is a functional optimized to reproduce properties of solids, the PZ-SIC brings the calculations into good agreement with the best *ab initio* estimates. The importance of using complex optimal orbitals becomes particularly clear in calculations using the TPSS functional, where the original functional gives good results while the application of PZ-SIC with real orbitals gives highly inaccurate results. With complex optimal orbitals, PZ-SIC slightly improves the accuracy of the TPSS functional. The charge localization problem that plagues Kohn–Sham DFT functionals, including hybrid functionals, is illustrated by calculations on the $CH_3 + F^-$ complex, where even PBEsol with PZ-SIC is found to give estimates of both energy and charge with accuracy comparable to that of coupled cluster calculations.

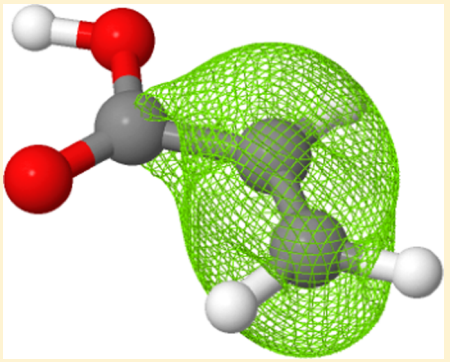

INTRODUCTION

Kohn–Sham density functional theory[1,2] (KS-DFT) is one of the most successful and widely used methods in computational chemistry and solid-state physics, because it successfully combines computational performance with sufficient accuracy for a wide variety of problems.[3,4] While the exact exchange-correlation (xc) functional that describes how electrons interact is not known, several approximations have been developed over the years. In contrast to wave-function-based methodology, KS-DFT lacks a systematic way to approach the exact solution to the electronic problem via successively better model Hamiltonians. However, the various approximate xc functionals can be placed onto rungs defined by their functional form:[5]

- functionals depending only on the local density, described using the local (spin) density approximation (LDA):[2,6]

$$E^{\mathrm{xc;LDA}} = \int n(\mathbf{r})\epsilon_{\mathrm{xc}}[n^{\alpha}(\mathbf{r}), n^{\beta}(\mathbf{r})]\,\mathrm{d}^3r \tag{1}$$

where ϵ_{xc} is the energy per electron and $n^{\sigma}(\mathbf{r})$ is the density of electrons with spin σ at point $\mathbf{r}$, with α and β denoting spin-up and spin-down, respectively.

- functionals depending on the local density and its gradient, described using the generalized-gradient approximation (GGA):[7]

$$E^{\mathrm{xc;GGA}} = \int n(\mathbf{r})\epsilon_{\mathrm{xc}}[n^{\alpha}(\mathbf{r}), n^{\beta}(\mathbf{r}), \nabla n^{\alpha}(\mathbf{r}), \nabla n^{\beta}(\mathbf{r})]\,\mathrm{d}^3r \tag{2}$$

- functionals depending on the local density, its gradient and its Laplacian, as well as the kinetic energy density, described using the meta-GGA approximation (mGGA)

$$E^{\mathrm{xc;mGGA}} = \int n(\mathbf{r})\epsilon_{\mathrm{xc}}[n^{\alpha}(\mathbf{r}), n^{\beta}(\mathbf{r}), \nabla n^{\alpha}(\mathbf{r}), \nabla n^{\beta}(\mathbf{r}), \nabla^2 n^{\alpha}(\mathbf{r}), \nabla^2 n^{\beta}(\mathbf{r}), \tau^{\alpha}(\mathbf{r}), \tau^{\beta}(\mathbf{r})]\,\mathrm{d}^3r \tag{3}$$

where τ^{σ} is the kinetic energy density for electrons of spin σ. Several functionals have also been developed where a fraction of exact (i.e., Hartree–Fock) exchange is added.[8,9]

However, despite the significant development in the functional form and the large number of proposed approximate functionals, several shortcomings remain, and even for some simple problems the predictions of functionals of all rungs are inaccurate. For example, practically all functionals fail to reproduce the simplest possible bond breaking $H_2^+ \rightarrow H + H^+$ (instead, one obtains $H^{0.5} + H^{0.5}$), and fail to predict bound anions[10] such as H^-. These problems have been identified as artifacts of self-interaction (SI) error in the approximate energy functionals, which typically leads to electrons spuriously repelling themselves. While the inclusion of gradient dependence in going from LDA to GGA significantly decreases the SI

Received: July 18, 2014

   dx.doi.org/10.1021/ct500637x | J. Chem. Theory Comput. XXXX, XXX, XXX–XXX

energy of core orbitals, the SI of valence orbitals is of similar magnitude on both rungs.[11,12]

For a single-electron density n_s, it can be shown[13] that the exact KS xc functional satisfies

$$E^{xc}[n_s] = -J[n_s] \tag{4}$$

where the Coulomb energy is

$$J[n] = \int\int \frac{n(\mathbf{r})n(\mathbf{r}')}{|\mathbf{r}-\mathbf{r}'|}\, d^3r\, d^3r' \tag{5}$$

However, approximate functionals violate eq 4, leaving an amount of SI error:

$$E^{SI}[n_s] = E^{xc}[n_s] + J[n_s] \tag{6}$$

For many-electron systems, Perdew and Zunger proposed an orbital-based SI correction that is accurate for single-electron systems but approximate for many-electron systems:[13]

$$E^{PZ}[n^\alpha, n^\beta] = E^{KS}[n^\alpha, n^\beta] - \sum_{i\sigma} (E^{xc}[n_i^\sigma] + J[n_i^\sigma]) \tag{7}$$

Here, n_i^σ is the density of spin-orbital i corresponding to spin σ, which is either α or β. Importantly, E^{PZ} reduces to E^{KS} for the exact E^{xc}.

While the energy given by KS energy functionals is independent of the representation used for the occupied orbitals, the second term in eq 7 clearly makes the Perdew–Zunger self-interaction correction (PZ-SIC) energy functional dependent on the choice of the representation of the occupied orbitals. That is, KS energy functionals are invariant under rotations in the occupied space, while functionals obtained after applying PZ-SIC are not. [Note that the SI energy is nonlinear: $\sum_{i\sigma}E^{SI}[n_i^\sigma] \neq \sum_\sigma E^{SI}[\sum_i n_i^\sigma]$.] Thus, a correction based on canonical orbitals will give a different result than one based on, e.g., Foster–Boys[14] or Edmiston–Ruedenberg (ER)[15] localized orbitals, both of which give an equally valid description of the system at the KS-DFT level of theory. Extended systems represent an extreme case where two possible ways to represent the total density are the delocal Bloch orbitals and the local Wannier orbitals. In the limit of an infinite system, the correction will vanish for Bloch orbitals but is finite for Wannier orbitals. This makes the application of PZ-SIC mathematically more challenging than that of KS-DFT. While canonical molecular orbitals (CMOs) can conveniently be chosen to carry out the KS-DFT calculation, the choice for the optimal molecular orbitals (OMOs) to perform PZ-SIC calculations requires an additional optimization.

Quantum chemical calculations should involve variational minimization of the energy functional (here E^{PZ}). Since E^{KS} is unitary invariant, the OMOs $i\sigma$ for PZ-SIC are determined by the requirement that the SI energy part in eq 7 be maximized (as proposed by Perdew and Zunger[13]). One can argue that the unitary invariance of the theory is then still maintained, if any rotation of the set of orbitals is accompanied by a counter-rotation to form the OMOs when the SI energy is evaluated.

Most of the previous implementations of PZ-SIC have not been variational, in that they have relied on some other scheme for forming local orbitals to evaluate the self-interaction energy than by finding the OMOs that minimize E^{PZ}. Localization can be achieved with a variety of objective functions. The oldest scheme is that of Foster and Boys,[14] in which the sum of orbital spreads is minimized. The solid-state analogue of the Foster–Boys scheme are the maximally localized Wannier functions.[19,20] A more-recent extension of the Foster–Boys scheme is the fourth moment method.[21] The objective function can also be taken to be the sum of magnitudes of partial charges of atoms, as in, i.e., the Pipek–Mezey method[22] and generalizations thereof.[23] Finally, maximization of the orbital self-Coulomb repulsion has also been used, as in the ER method,[15] and the orbital density self-overlap in the von Niessen method.[24] While the orbitals obtained with the various localization criteria are often similar, they are not the same, and can be expected to lead to different SI energies. Of these, the ER method is the closest one to PZ-SIC, since both contain the orbital self-Coulomb repulsion, but the appearance of the xc term in the PZ-SIC method results in significant differences because of the partial cancellation of these two terms in approximate xc functionals.

For infinite systems, a plane-wave solution obtained from the LDA functional is also a solution for the PZ-SIC LDA functional. Thus, PZ-SIC LDA is "exact" for the homogeneous electron gas, just as LDA is.[16−18] Variational optimization of the PZ-SIC energy can give either localized orbitals (e.g., a valence band) or delocal orbitals (a conduction band). Condensed phases represented by infinite models are no more difficult *a priori* than molecules; delocal as well as local orbitals may occur in both cases.

As a side note, Hartree–Fock (HF) theory is unitary invariant. This is seen explicitly in the conventional formulation of the theory, where a SI term is added to the Coulomb and exchange contributions, so that both then are dependent only on the total density. [To obtain the total density, the diagonal term must be added to the Coulomb interaction $\sum_{j>i} r_{ij}^{-1}$.] This can be done, because the SI terms introduced in the Coulomb and exchange cancel each other out. In contrast, Hartree theory[25−27] is not unitary invariant, because the fermionic exchange term is not included. Hartree theory can be obtained from a variational implementation of PZ-SIC simply by omitting exchange and correlation from the calculation.

While the original formulation of PZ-SIC implies that the occupied orbitals must be solved with different Hamiltonians, Harrison, Heaton, and Lin, shortly after the publication of the article by Perdew and Zunger,[13] showed that a common, unified Hamiltonian (UH) for all the orbitals in the system can easily be obtained.[28] This clarifies the role of the orbital-dependent potentials that arise from eq 7. The UH approach guarantees orthonormal orbitals and can be used to divide the problem of solving for the electronic structure into an optimization of the CMOs and an optimization of the OMOs. Nevertheless, several implementations of PZ-SIC have not made use of the UH, but rather relied on approaches reminiscient of the one originally proposed by Perdew and Zunger.[29]

One problem with the UH approach is that it is not clear what Hamiltonian should be used for the virtual orbitals. This can be solved by using the optimized effective potential (OEP) approach.[30,31] Applied on PZ-SIC, the OEP yields the correct asymptotic behavior for the potential, as can be seen from the following argument. In regions where the total electron density is dominated by a single orbital k, $n_k(\mathbf{r}) \gg n_i(\mathbf{r}) \forall i \neq k$, the OEP will coincide with the potential of that orbital. Assuming that k is the highest occupied orbital, the potential is asymptotically given by the Coulomb potential of the nuclei with charge Z and the $Z - Q$ other electrons in the system, giving a total potential energy $-Q/r$ seen by the outermost electron, with Q being the total charge of the system. In contrast, the KS-DFT potential

dx.doi.org/10.1021/ct500637x | J. Chem. Theory Comput. XXXX, XXX, XXX−XXX

contains a SI contribution that violates the correct r^{-1} behavior. However, constructing the exact OEP is computationally costly and numerically unstable, so an approximation by Krieger, Li, and Iafrate[32,33] (KLI) is typically used instead. However, even the KLI approach remains computationally costly.[34] The use of the KLI potential has been shown to bring the ionization energy as given by the highest occupied orbital energy eigenvalue,[35] $-\epsilon_{\max}$ (which is already good in PZ-SIC), closer to the experimental value.[36] While the long-range form of the potential obtained from GGA functionals is far from correct and virtual states are even qualitatively incorrect, the application of PZ-SIC to these approximate functionals and construction of the KLI OEP (which has the right asymptotic form, as discussed above) gives quite an accurate description of even Rydberg excited states of molecules, as has been recently shown.[37−39]

For many-electron systems, the PZ-SIC functionals are not self-interaction free. The orbital-based estimate is only an approximation. It has been pointed out by Lundin and Eriksson[40] (LE) that the application of PZ-SIC to approximate xc functionals leaves residual SI because of the nonlinearity of the xc functionals $[V(\overline{n} + n_i) - V(n_i) \neq V(\overline{n})]$, and they suggest an approach for correcting the density rather than the potentials. It is, however, not clear that the LE scheme fulfills the same appealing properties of PZ-SIC mentioned above. Also, the scheme has not been fully developed and tested.[41] As PZ-SIC, the LE scheme will break unitary invariance and thus require unitary optimization to determine the orbitals. But, the unitary optimization may be easier in an LE scheme than in the PZ-SIC scheme, as the potentials addressed in the latter scheme can diverge at orbital nodes, whereas the former scheme is based on background densities which are expected to be significantly smoother. A large part of the algorithm presented here for the PZ-SIC scheme should also be applicable to the LE scheme.

Recently, several implementations of PZ-SIC have been made available. Most of these are nonvariational, approximate implementations based on Foster−Boys orbitals: for example, those in COLOGNE 2003,[42,43] NWCHEM,[34,44] and ADF,[11,45,46] where the latter two make use of the KLI approximation in the implementation. Also, an *ad hoc* correction based on atomic orbitals is available in SIESTA.[47] A variational, self-consistent implementation has been implemented in a branch of GAUSSIAN.[12,48]

The performance of the PZ-SIC has been extensively been studied by Harrison and co-workers,[28,49−54] Heaton and co-workers,[55−60] and Pederson and co-workers.[17,61−65] Molecular properties have been studied by several groups.[11,34,42−46] More-recent benchmarks have been carried out by Vydrov and Scuseria,[12] who found that an overcorrection to GGA density functionals is often obtained and suggested scaling down the correction in the valence region.[66,67] All of these and other previous applications of PZ-SIC have made use of real orbitals only. However, it has recently been shown that it is essential to use complex OMOs with PZ-SIC. While PZ-SIC applied to GGA functionals with real OMOs can lead to reduced accuracy of the energy of atoms and molecules, the accuracy is typically improved when complex OMOs are used.[68,69] Therefore, the previous tests need to be re-evaluated. For further information about the PZ-SIC, the reader is referred to a recent review by Pederson and Perdew.[70] A more general review on SI corrections has been recently written by Tsuneda and Hirao.[71]

The organization of the manuscript is the following. Next, in the Theory section, we will discuss the equations necessary to implement PZ-SIC within a basis set approach. Then, in the Implementation section, we discuss the current implementation in more detail, followed by the Results section. The article concludes with a Summary and Discussion section. Atomic units are used throughout, unless otherwise stated.

THEORY

Kohn−Sham Density Functional Theory (KS-DFT). The energy functional in KS-DFT is usually written as

$$E^{\mathrm{KS}}[n] = T_s[n] + V[n] + J[n] + K[n] \tag{8}$$

where $T_s[n]$ represents the kinetic energy,

$$T_s[n] = -\frac{1}{2}\sum_{\sigma}\sum_{I=1}^{N^\sigma}\langle\phi_I^\sigma|\nabla^2|\phi_I^\sigma\rangle \tag{9}$$

$V[n]$ is the external potential energy,

$$V[n] = \int n(\mathbf{r})V(\mathbf{r})\,\mathrm{d}^3r \tag{10}$$

$J[n]$ is the Coulomb repulsion energy,

$$J[n] = \frac{1}{2}\iint\frac{n(\mathbf{r})n(\mathbf{r}')}{|\mathbf{r}-\mathbf{r}'|}\,\mathrm{d}^3r\,\mathrm{d}^3r' \tag{11}$$

and $K[n]$ is the xc energy,

$$K[n] = \int f_{\mathrm{xc}}(n^\alpha(\mathbf{r}), n^\beta(\mathbf{r}), \gamma^{\alpha\alpha}(\mathbf{r}), \gamma^{\alpha\beta}(\mathbf{r}), \gamma^{\beta\beta}(\mathbf{r}), \nabla^2 n^\alpha(\mathbf{r}), \nabla^2 n^\beta(\mathbf{r}), \tau^\alpha(\mathbf{r}), \tau^\beta(\mathbf{r}))\,\mathrm{d}^3r \tag{12}$$

taken here in the meta-generalized-gradient form, with the commonly used shorthand $f_{xc}(n) := n\epsilon_{xc}(n)$. The density of electrons with spin σ is spanned by the N^σ occupied CMOs ϕ_I^σ,

$$n^\sigma(\mathbf{r}) = \sum_{I=1}^{N^\sigma}|\phi_I^\sigma(\mathbf{r})|^2 \tag{13}$$

and the total electron density is simply

$$n(\mathbf{r}) = n^\alpha(\mathbf{r}) + n^\beta(\mathbf{r}) \tag{14}$$

The reduced gradient expressions in eq 12 are given by

$$\gamma^{\sigma\sigma'}(\mathbf{r}) = \nabla n^\sigma(\mathbf{r})\cdot\nabla n^{\sigma'}(\mathbf{r}) \tag{15}$$

and the kinetic energy density is

$$\tau^\sigma(\mathbf{r}) = \frac{1}{2}\sum_{I=1}^{N^\sigma}|\nabla\phi_I^\sigma(\mathbf{r})|^2 \tag{16}$$

The minimization of the KS-DFT energy functional $E[n]$ with the constraint of orthonormal orbitals in a finite basis set leads to algebraic self-consistent field (SCF) equations of the Pople−Nesbet−Roothaan−Hall[72,73] type

$$\mathbf{F}^\sigma\mathbf{C}^\sigma = \mathbf{S}\mathbf{C}^\sigma\mathbf{E}^\sigma \tag{17}$$

as discussed in ref 74. Here, $\mathbf{S}$ is the overlap matrix, $S_{\mu\nu} = \langle\mu|\nu\rangle$, $\mathbf{C}^\sigma$ is a matrix containing the CMO coefficients, and $\mathbf{E}^\sigma$ is a diagonal matrix holding the orbital energy eigenvalues. The electron density is written as

$$n^\sigma(\mathbf{r}) = \sum_{\mu\nu=1}^{K}P_{\mu\nu}^\sigma\chi_\mu^*(\mathbf{r})\chi_\nu(\mathbf{r}) \tag{18}$$

where the density matrix is given by

$$\mathbf{P}^{\sigma} = \sum_{I=1}^{N^{\sigma}} \mathbf{C}_I \mathbf{C}_I^{\dagger} \tag{19}$$

Here, $\mathbf{C}_I$ is the Ith column of $\mathbf{C}$, containing the coefficients of the CMO I. K in eq 18 denotes the number of functions in the basis set. The Kohn−Sham−Fock matrix $\mathbf{F}^{\sigma} = \partial E^{\mathrm{KS}}/\partial \mathbf{P}^{\sigma}$ appearing in eq 17 is given by

$$\mathbf{F}^{\sigma} = \mathbf{H}^{\mathrm{core}} + \mathbf{J} + \mathbf{K}^{\sigma} \tag{20}$$

where the core Hamiltonian has matrix elements

$$H_{\mu\nu}^{\mathrm{core}} = \left\langle \mu \left| -\frac{1}{2}\nabla^2 \right| \nu \right\rangle - \sum_{\text{nuclei A}} Z_{\mathrm{A}} \int \frac{\chi_{\mu}(\mathbf{r})\chi_{\nu}(\mathbf{r})}{|\mathbf{r} - \mathbf{r}_{\mathrm{A}}|}\, \mathrm{d}^3 r \tag{21}$$

the Coulomb matrix is

$$J_{\mu\nu} = \sum_{\tau\upsilon=1}^{K} (\mu\nu|\tau\upsilon) P_{\tau\upsilon} \tag{22}$$

where the electron repulsion integral is given by

$$(\mu\nu|\tau\upsilon) = \int\int \frac{\chi_{\mu}^{*}(\mathbf{r})\chi_{\nu}(\mathbf{r})\chi_{\tau}^{*}(\mathbf{r}')\chi_{\upsilon}(\mathbf{r}')}{|\mathbf{r} - \mathbf{r}'|}\, \mathrm{d}^3 r\, \mathrm{d}^3 r' \tag{23}$$

and the xc matrix has elements

$$K_{\mu\nu}^{\sigma} = \int \left[\frac{\delta f_{\mathrm{xc}}}{\delta n^{\sigma}} \chi_{\mu}^{*}\chi_{\nu} + \left(2\frac{\delta f_{\mathrm{xc}}}{\delta \gamma^{\sigma\sigma}} \nabla n^{\sigma} + \frac{\delta f_{\mathrm{xc}}}{\delta \gamma^{\sigma\sigma'}} \nabla n^{\sigma'} \right) \cdot \nabla(\chi_{\mu}^{*}\chi_{\nu}) + \frac{1}{2}\frac{\delta f_{\mathrm{xc}}}{\delta \tau^{\sigma}} \nabla\chi_{\mu}^{*} \cdot \nabla\chi_{\nu} + \frac{\delta f_{\mathrm{xc}}}{\delta(\nabla^2 n^{\sigma})} \nabla^2(\chi_{\mu}^{*}\chi_{\nu}) \right] \mathrm{d}^3 r \tag{24}$$

where $\sigma' \neq \sigma$.

PZ-SIC. As already discussed in the Introduction (eq 7), in the PZ-SIC scheme, an estimate of the SI is explicitly subtracted from the KS functional

$$E^{\mathrm{PZ}}[n] = E^{\mathrm{KS}}[n] - E^{\mathrm{SI}}[n] \tag{25}$$

where the SI energy is obtained orbital by orbital,

$$E^{\mathrm{SI}}[n] = \sum_{i\sigma} \left(J[n_i^{\sigma}] + E^{\mathrm{xc}}[n_i^{\sigma}] \right) \tag{26}$$

with

$$n_i^{\sigma}(\mathbf{r}) = |\psi_i^{\sigma}(\mathbf{r})|^2 \tag{27}$$

Together, the occupied orbitals span the total density:

$$\sum_{i=1}^{N^{\sigma}} n_i^{\sigma}(\mathbf{r}) = n^{\sigma}(\mathbf{r}) \tag{28}$$

It is important to note that *these orbitals are not defined a priori* but should rather be found by variational calculations, resulting in the OMOs. Because of eq 28, the OMOs must be expressable in terms of the occupied CMOs as

$$|\psi_i^{\sigma}\rangle = \sum_{I=1}^{N^{\sigma}} |\phi_I^{\sigma}\rangle W_{Ii}^{\sigma} \tag{29}$$

with $(\mathbf{W}^{\sigma})^{\dagger}\mathbf{W}^{\sigma} = \mathbf{1} = \mathbf{W}^{\sigma}(\mathbf{W}^{\sigma})^{\dagger}$. A generalization of eq 29 to fractionally occupied orbitals has been presented elsewhere.[60]

Effect on the Wave Function. After inclusion of PZ-SIC, the SCF equations (eq 17) become

$$\mathbf{F}^{\sigma}\mathbf{C}_{\mathrm{occ}}^{\sigma} - \left(\sum_{i=1}^{N^{\sigma}} \mathbf{f}_i^{\sigma}\mathbf{p}_i^{\sigma} \right) \mathbf{S}\mathbf{C}_{\mathrm{occ}}^{\sigma} = \mathbf{S}\mathbf{C}_{\mathrm{occ}}^{\sigma}\mathbf{E}_{\mathrm{occ}}^{\sigma} \tag{30}$$

$$\mathbf{F}^{\sigma}\mathbf{C}_{\mathrm{virt}}^{\sigma} = \mathbf{S}\mathbf{C}_{\mathrm{virt}}^{\sigma}\mathbf{E}_{\mathrm{virt}}^{\sigma} \tag{31}$$

where

$$\mathbf{f}_i^{\sigma} = \mathbf{J}(\mathbf{p}_i^{\sigma}) + \mathbf{K}(\mathbf{p}_i^{\sigma}) \tag{32}$$

denotes the KS-Fock matrix arising from the ith OMO density matrix $\mathbf{p}_i^{\sigma}$, with $\mathbf{J}$ and $\mathbf{K}$ being given by eqs 22 and 24, respectively, and occ and virt refer to the occupied and virtual blocks. The OMO density matrix is simply

$$\mathbf{p}_i^{\sigma} = \mathbf{c}_i^{\sigma}(\mathbf{c}_i^{\sigma})^{\dagger} \tag{33}$$

where the OMO coefficients $\mathbf{c}_i^{\sigma}$ can be written in terms of the occupied CMO coefficients (eq 29) as

$$\mathbf{c}_i^{\sigma} = \sum_{J=1}^{N^{\sigma}} \mathbf{C}_J^{\sigma} W_{Ji}^{\sigma} \tag{34}$$

The form of eqs 30 and 31 would suggest that the occupied orbitals and the virtual orbitals must be solved separately. But then, a self-consistent solution of the equations would be impossible: an improvement to the total density requires mixing of occupied and virtual orbitals until the occupied-virtual and virtual-occupied blocks of the electronic gradient vanish.[75] However, from the form of the additional term in the occupied space, it can be seen that the SIC simply acts as a level shift[76] for the occupied orbitals, pulling them down or pushing them up in energy. The same term can also be inserted in the virtual space, because $\mathbf{p}_i^{\sigma}\mathbf{S}\mathbf{C}_{\mathrm{virt}}^{\sigma} = \mathbf{0}$ by orthogonality of the occupied and virtual spaces. Thus, the SIC-SCF equation can be written as

$$(\mathbf{F}^{\sigma} + \mathbf{F}_{\mathrm{SIC}}^{\sigma})\mathbf{C}^{\sigma} = \mathbf{S}\mathbf{C}^{\sigma}\mathbf{E}^{\sigma} \tag{35}$$

where $\mathbf{F}_{\mathrm{SIC}}^{\sigma}$ is an effective potential, given by

$$\mathbf{F}_{\mathrm{SIC}}^{\sigma} = -\left(\sum_{i=1}^{N^{\sigma}} \mathbf{f}_i^{\sigma}\mathbf{p}_i^{\sigma} \right) \mathbf{S} \tag{36}$$

This term is not symmetric, so we have opted to symmetrize it by hand, to restore meaningful CMOs and orbital energies, yielding

$$\mathbf{F}_{\mathrm{SIC}}^{\sigma} = -\frac{1}{2} \sum_{i=1}^{N^{\sigma}} (\mathbf{f}_i^{\sigma}\mathbf{p}_i^{\sigma}\mathbf{S} + \mathbf{S}\mathbf{p}_i^{\sigma}\mathbf{f}_i^{\sigma}) \tag{37}$$

as has also been done by Heaton, Harrison, and Lin.[56] It has been shown that this approach is equivalent to neglecting the off-diagonal Lagrange multipliers, which are usually small.[28] Note that another UH that treats the off-diagonal multipliers accurately has also been suggested in the literature.[28] It can be written as

$$\mathbf{F}_{\mathrm{SIC}}^{\sigma} = -\mathbf{S} \sum_{i=1}^{N^{\sigma}} (\mathbf{p}_i^{\sigma}\mathbf{f}_i^{\sigma}\mathbf{p}_i^{\sigma} + \mathbf{v}^{\sigma}\mathbf{f}_i^{\sigma}\mathbf{p}_i^{\sigma} + \mathbf{p}_i^{\sigma}\mathbf{f}_i^{\sigma}\mathbf{v}^{\sigma})\mathbf{S} \tag{38}$$

where the virtual space projector is

$$\mathbf{v}^{\sigma} = \sum_{\text{virtual } I} \mathbf{C}_I^{\sigma}(\mathbf{C}_I^{\sigma})^{\dagger} \tag{39}$$

dx.doi.org/10.1021/ct500637x | J. Chem. Theory Comput. XXXX, XXX, XXX−XXX

While both Hamiltonians (eqs 37 and 38) are available in the PZ-SIC implementation in ERKALE, all of the calculations presented here are based on the former, symmetrized Hamiltonian.

Both forms of the UH given above only affect the occupied orbitals, usually by pulling them down in energy and changing their shape, while the virtual orbitals are only affected indirectly through their orthogonality to the occupied orbitals. Thus, the band gap between the highest occupied molecular orbital (HOMO) and the lowest unoccupied molecular orbital (LUMO) is typically increased, as the HOMO energy is reduced but the LUMO energy remains approximately constant.

However, it is clear that the virtual orbitals and their orbital energies should also be corrected to reflect the correct asymptotic form of the potential. It has been shown that atomic excitations can be modeled by the addition of an extra term

$$\mathbf{F}^{\sigma}_{\mathrm{SIC;virtual}} = -\mathbf{S}\mathbf{v}^{\sigma}\mathbf{f}^{\sigma}_{i}\mathbf{v}^{\sigma} \tag{40}$$

where (i, σ) is the spin-orbital from which the excitation occurs.[28] This term only affects the virtual space but requires one to be able to identify the initial state, which may not be straightforward in molecules, especially when excitations can occur from various initial states. As discussed in the Introduction, a better defined alternative is to use an OEP (usually in the KLI approximation), with which a single effective potential $V^{\mathrm{OEP}}(\mathbf{r})$ common to *all* of the orbitals (occupied and virtual) is obtained.

Unitary Optimization of Orbitals. In the present implementation, the unitary optimization is performed using a recently proposed algorithm,[77,78] which we have previously found[79] to be computationally efficient for ER localization.[15] During the unitary optimization, the SI energy is maximized while keeping the total density fixed. Because this optimization is done separately for both spin channels, we will drop the spin indices in the discussion that follows. The task now is to optimize $\mathbf{W}$ in eq 34. Since the algorithms used to perform the unitary optimization are discussed extensively elsewhere,[77−79] only a brief summary is presented here.

The Euclidean derivative of the SI energy needed for the unitary optimization is

$$\Gamma = \frac{\partial E^{\mathrm{SI}}}{\partial W^{*}_{Ab}} = \mathbf{C}^{\dagger}_{A}\mathbf{f}_{b}\mathbf{c}_{b} \tag{41}$$

The expression given in eq 41 is analogous to ER localization, where the Coulomb matrix $\mathbf{J}(\mathbf{p}_b)$ appears instead of the full Kohn−Sham−Fock matrix.[79] Also, an analogous result to eq 41 has been presented previously for the LDA level of theory.[80] It is, however, at variance with that of Hoffman et al.[81] (see eq (B4) in their work).

The unitary gradient is given by[77,78]

$$\mathbf{G} = \mathbf{\Gamma}\mathbf{W}^{\dagger} - \mathbf{W}\mathbf{\Gamma}^{\dagger} \tag{42}$$

Starting from an initial guess for $\mathbf{W}$, the iteration consists of computing a new search direction $\mathbf{G}$ and maximizing E^{SI} along the line

$$E^{\mathrm{SI}}(\mu) = E^{\mathrm{SI}}(\mathbf{W}_k \mathrm{e}^{-\mu\mathbf{G}_k}) \tag{43}$$

A conjugate gradient method is used to update the search direction and the line minimization is performed by fitting a third-order polynomial to the analytic derivative of E^{SI} to find its smallest positive zero.[78]

The unitary optimization is continued until the elements of the anti-Hermitian matrix,

$$\kappa_{ij} = \mathbf{c}^{\dagger}_{i}(\mathbf{f}_{j} - \mathbf{f}_{i})\mathbf{c}_{j} \tag{44}$$

drop below the tolerance threshold. By calculus of variations, it is easily shown that the matrix $\boldsymbol{\kappa}$ vanishes at the extrema of the SI energy. However, in practice, it is hard to satisfy $\boldsymbol{\kappa} = \mathbf{0}$ exactly. But, it will be shown below in the Results section that this is not necessary as convergence of the full procedure can still be obtained with a finite value of $\boldsymbol{\kappa}$. This is easily understood because of the variational nature of the present approach: small errors in the minimization should not result in large errors in the calculation. (The same rationale also explains why approximate OMOs such as those obtained from the Foster−Boys procedure may yield acceptable results.)

Simplification to Real Densities. The OMOs are generally complex. Correspondingly, the orbital density matrix (eq 33) is complex. However, in a pure DFT functional, all of the terms are dependent only on the electron density, which is real. [A pure DFT functional is a functional that only depends on the density and its derivatives; there is no contribution from exact exchange.] If the basis functions $\{\chi_\mu\}$ also are real, the orbital density can be written as

$$\begin{aligned} n^{\sigma}_{i}(\mathbf{r}) &= \Big(\sum_{\mu} c^{\sigma}_{\mu i}\chi_{\mu}(\mathbf{r})\Big)\Big(\sum_{\nu} (c^{\sigma}_{\nu i})^{*}\chi_{\nu}(\mathbf{r})\Big) \\ &= \sum_{\mu\nu} (\mathrm{Re}\; c^{\sigma}_{\mu i}(c^{\sigma}_{\nu i})^{*})\chi_{\mu}(\mathbf{r})\chi_{\nu}(\mathbf{r}) \end{aligned} \tag{45}$$

where Re denotes the real part. From here, a simpler form for the orbital density matrix (eq 33) can be identified as

$$\mathbf{p}^{\sigma}_{i} = \mathrm{Re}\; \mathbf{c}^{\sigma}_{i}(\mathbf{c}^{\sigma}_{i})^{\dagger} \tag{46}$$

Then, the orbital SI Fock matrices (eq 32) will also be real.

Now, the correction to the full Fock matrix (eq 37 or eq 38) will still be complex, because of the contribution from the complex orbital density matrix (eq 33). However, as found in ref 68, the CMOs turn out to have a similar shape in the complex and the real treatments. Here, we introduce an approximation where the imaginary part of $\mathbf{F}^{\mathrm{SIC}}$ is ignored, after which the CMOs can be chosen to be real. The approximation should be quite accurate, as the CMOs are only used to represent the electron density, which is real, and as a complex representation is still used to construct the optimal orbital densities. Within this approximation the PZ-SIC algorithm can easily be incorporated into existing KS-DFT programs using real algebra.

The validity of the approximation can even be easily tested. Let $\mathbf{C}^{\sigma}$ contain the orbitals arising from the real part of $\mathbf{F}^{\sigma} + \mathbf{F}^{\sigma}_{\mathrm{SIC}}$, and $\tilde{\mathbf{C}}^{\sigma}$ the orbitals from the full, complex operator. Computing the overlap of these vectors

$$O_{IJ} = (\mathbf{C}^{\sigma}_{I})^{\mathrm{T}}\mathbf{S}\tilde{\mathbf{C}}^{\sigma}_{J} \tag{47}$$

gives the fraction of the occupied density subspace lost in the approximation as

$$\delta = 1 - \sum_{I,J=1}^{N^{\sigma}} |O_{IJ}|^{2} \tag{48}$$

dx.doi.org/10.1021/ct500637x | J. Chem. Theory Comput. XXXX, XXX, XXX−XXX

the calculation of which only requires the diagonalization of a single complex Fock matrix. In all of the calculations performed in the present manuscript, $\delta \leq O(10^{-5})$, verifying the validity of the approximation.

However, if a functional containing part of exact exchange (e.g., a hybrid functional) is used, the entire SCF procedure needs to be complex, because imaginary parts will be carried to the off-diagonal elements of the exchange matrix.[82,83] Even in this case, incorporation of the PZ-SIC procedure into an existing KS-DFT program is simple, provided it already can perform SCF calculations with complex orbitals. However, the PZ-SIC rectifies the deficiencies that one usually tries to address by the use of hybrid functionals, so there is little interest in a PZ-SIC scheme utilizing hybrid functionals.

Two-Step Self-Consistent Procedure. As stated previously in the PZ-SIC section, solving for the OMOs requires minimizing the functional $E^{\mathrm{PZ}}[n] = E^{\mathrm{KS}}[n] - E^{\mathrm{SI}}[n]$. The minimization of the first term essentially involves of a self-consistent field (SCF) calculation, while the second term requires unitary optimizations to find the best rotations $\{\mathbf{W}^\sigma\}$. While it might be appealing to perform both operations simultaneously (minimize E^{KS} and maximize E^{SI}), as has been done in the previous implementations,[12,42] this turns out to be problematic for several reasons.

First, maximizing E^{SI} is computationally much more expensive than minimizing E^{KS}, which, in essence, entails the solution of the SCF problem in a fixed external potential (given here by treating $-E^{\mathrm{SI}}[n]$ as fixed). An SCF calculation typically converges within a dozen iterations, requiring the same amount of Fock matrix builds. In contrast, *every point* of the unitary optimization requires computing N orbital-dependent Fock matrices, each of which has a cost comparable to a single step in an SCF calculation. Furthermore, in the present scheme, with the line search performed with a fit to a third-order polynomial, every step of the unitary optimization requires evaluating the matrices at four points, and many steps need to be taken for the unitary optimization itself to converge to the maximum E^{SI}.

Second, the solution of the SCF is a difficult nonlinear problem for which powerful algorithms have been developed. Changing the SIC term during the SCF iteration would couple the errors in the SIC term and the SCF, making *both* harder to converge. Again, since the computational effort in solving the SCF equation (eq 35) with fixed $\mathbf{F}^\sigma_{\mathrm{SIC}}$ is trivial, since only the total density is considered in this part, it is anyway computationally more efficient to handle the two tasks separately.

Conceptually, the difference between the two approaches of solving the PZ-SIC wave function can be illustrated as follows. Because evaluating orbital rotation Hessians is extremely costly, the usual approach for minimizing the PZ-SIC energy by simultaneous optimization of both the total density and the OMOs is based on a gradient descent method.[12,29] The true gradient of the PZ-SIC energy functional, with respect to orbital rotations, can be written as

$$\mathbf{G} = \begin{pmatrix} \mathbf{G}_{\mathrm{oo}} & \mathbf{G}_{\mathrm{ov}} \\ -\mathbf{G}_{\mathrm{ov}} & \mathbf{0} \end{pmatrix} \tag{49}$$

where $\mathbf{G}_{\mathrm{oo}} = \boldsymbol{\Gamma}$ is the gradient for the occupied-occupied (oo) rotations, $\mathbf{G}_{\mathrm{ov}}$ is the gradient for the occupied-virtual (ov) rotations, and the energy is invariant under rotations in the virtual−virtual block. Simultaneous optimization of the total density and the OMOs entails using the entire rotation gradient $\mathbf{G}$, whereas our suggestion is to perform subspace minimizations of the oo, and the ov and vo blocks separately. While the present scheme still uses a gradient method to perform the oo block optimization, it does not state *how* the ov and vo blocks are handled, because this part is performed by an SCF convergence routine. Recent progress on convergence accelerators[84−89] has significantly accelerated the solution of the SCF equations, compared to simpler gradient-descent-based methods, and fast SCF convergence is typically observed with modern accelerator algorithms. Again, by separating the two tasks, the effect of the PZ-SIC can be written as a modification to the one-electron core Hamiltonian, similar to the ones obtained, e.g., when core electrons are replaced with effective core potentials. This means that minimal changes to existing KS-DFT programs are necessary to implement the two-step self-consistent PZ-SIC procedure.

The implementation of the two-level scheme has been as follows: first, the SI energy is maximized, yielding a set of OMOs $i\sigma$, corresponding to fixed density n^σ. Second, the effect of the SIC potential is calculated (eq 37), after which improved orbitals are obtained by a SCF procedure with a fixed SIC potential term (eq 35). Self-consistency can then be achieved by repetition of the two steps. This process is illustrated in Figure 1.

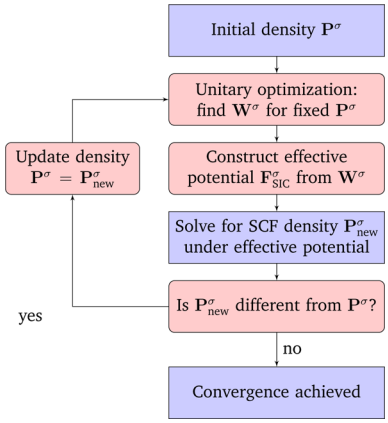

Figure 1. Flow diagram for the two-step self-consistent PZ-SIC algorithm presented here. The steps included in a KS-DFT calculation are shown in blue boxes, whereas the steps pertaining to PZ-SIC are shown in red boxes.

The error in the solution can be split into three parts. The first two are the error in the OMOs $i\sigma$ corresponding to density n^σ, and the error in the density n^σ for a fixed SIC term. The first error is related to how well the optimal rotation within the occupied space has been found, while the second tells how well the occupied space is converged with a given, fixed correction. Of these, the second is made negligible by modern SCF convergence accelerator techniques, but the first error is harder to reduce. Fortunately, the variational nature of the present method allows for slight inaccuracies in the minimization. The third type of error is related to the compound procedure: how much the density changes upon successive refinement of both $i\sigma$ and n^σ.

Because the SIC term only acts on the occupied space, a simple fixed-point iteration is expected to converge, in contrast to the case of SCF iteration, where it usually diverges, since SCF iteration entails mixing occupied and virtual orbitals. However, in cases where some orbitals have a positive SIC, they

dx.doi.org/10.1021/ct500637x | J. Chem. Theory Comput. XXXX, XXX, XXX−XXX

may be pushed higher in energy, which can then cause oscillations in the orbital occupations from one SIC self-consistency iteration to another. In these cases, the application of eq 35 will probably fail, at least when the iterations are not damped. A better procedure for such a case is the application of the KLI-OEP approach for the virtual orbitals, thus resulting in a more consistent treatment of all the states in the system. When the two-step method proposed here converges, the correction to the virtual orbitals can be made subsequently within the KLI-OEP approach in a single step by using the converged occupied orbitals.

We have seen that the two-step procedure may fail to converge when small basis sets are used. For instance, the calculation on the F atom failed to converge with the cc-pVDZ basis, but converged without problems with larger basis sets. We believe the reason to be the following. The two-step procedure of minimizing $E^{\mathrm{PZ}}[n] = E^{\mathrm{KS}}[n] - E^{\mathrm{SI}}[n]$ relies on PZ-SIC being a small correction to the total electronic structure. However, with small basis sets, there is little variational freedom to determine the optimal density. To achieve the true minimum of E^{PZ}, it may be necessary to optimize both the canonical orbitals and the localizing matrices simultaneously, possibly necessitating even a second-order (e.g., Newton–Raphson) procedure.

It is possible that the two-step procedure and the combined optimization converge to different solutions. They can also converge to a saddle point, as is the case for any SCF calculation. Since both the combined optimization scheme and the two-step SCF scheme are based on first-order methods for the minimization of E^{PZ}, they can be expected *a priori* to have similar problems with saddle point convergence. In both cases, a stability analysis[90,91] of the wave function with respect to concurrent rotations in the oo and ov blocks would be necessary, but this tends to be computationally demanding, even in the KS-DFT case. We are not aware of any work in this direction for PZ-SIC. In any case, the two-step process is a good way to get close to the optimal solution. Subsequently, one could switch to a combined optimization of both the orbitals and the localizing matrix.

IMPLEMENTATION

The procedure presented above has been implemented in the freely available ERKALE quantum chemistry program.[92,93] The xc functionals are evaluated in ERKALE with the libxc library,[94,95] which provides a large selection of commonly used functionals. ERKALE currently supports functionals at the LDA, GGA, and mGGA levels of theory. While ERKALE also supports hybrid functionals,[8,9] as was mentioned in the Theory section, the treatment of exact exchange in the SIC formalism would require a complex SCF algorithm, which is currently not implemented in ERKALE.

All of the results presented in the present manuscript have been obtained by evaluating the Coulomb matrices (eq 22) using density fitting[96,97] with an automatically generated fitting basis.[98] The SCF calculations are started from a superposition of atomic densities,[99] and the SCF convergence is accelerated by a combination of the ADIIS[89] [augmented Roothaan–Hall energy DIIS] and DIIS[84,85] [direct inversion in the iterative subspace] methods.

As discussed in ref 79, converging onto a complex matrix requires a complex starting point for the optimization. In the present work, we have started the calculations from a random unitary matrix (for calculations with complex orbitals) or a random orthogonal matrix (for calculations with real orbitals). Because of the similarities of the unitary optimization with conventional orbital localization methods, the PZ-SIC calculation is initialized first by a Pipek–Mezey (PM) localization using IAO charges,[22,23,100] and then further refined with a sloppy Edmiston–Ruedenberg (ER) localization[15] (see below for the criteria used). This procedure provides a cost-effective starting point for the maximization of the full SI energy. It is important not to take the ER localization too far because of the competition between the Coulomb and xc energy contributions to the SI energy: a tight optimization of the Coulomb part may lead to spurious saddle point convergence in the unitary optimization.

The PM and ER based localization calculation is only performed in the first unitary optimization cycle. In successive unitary optimizations, the optimization is started from a projection of the OMOs of the preceding cycle:

$$\mathbf{W} = \mathrm{unitarize}[(\mathbf{C}_{\mathrm{occ}}^{\mathrm{new}})^{\dagger}\mathbf{S}(\mathbf{C}_{\mathrm{occ}}^{\mathrm{old}}\mathbf{W}^{\mathrm{old}})] \tag{50}$$

The projection of the OMOs is used instead of the preceding matrix $\mathbf{W}$, as rotations in the oo space of the CMOs can take place in the SCF cycle. Also, the projection must be reunitarized, because of ov mixing in the SCF. This is performed in ERKALE by a singular value decomposition, followed by setting all of the singular values to unity.

The unitary optimization of the localizing matrix $\mathbf{W}^{\sigma}$ and the computation of the effective potential $\mathbf{F}_{\mathrm{SIC}}^{\sigma}$ require a numerical grid for the integration of the xc potential. Because the orbital densities are not as smooth as the total density, grids parametrized for KS-DFT calculations should not be used for PZ-SIC. In the present work, we have solved this problem by extending the adaptive grid generator proposed by Köster et al.[101] to produce a grid that integrates all of the orbital potentials (i.e., the diagonal elements of the xc matrices $\mathbf{K}(\mathbf{p}_i)$ within the wanted accuracy τ. A new grid is generated at the start of every unitary optimization cycle. The resulting integration grids for the unitary optimization are 2–3 times larger than those used for the SCF procedure. The larger grid requirement of PZ-SIC, compared to KS-DFT, has also been noted by other authors.[12,45] In the present work, the accuracy thresholds $\tau_{\mathrm{initial}} = 10^{-4}$ and $\tau_{\mathrm{final}} = 10^{-5}$ for the diagonal elements of the KS-Fock matrix have been used.[93,101] The program switches to the final threshold after full self-consistency has been achieved with the initial grid threshold.

The convergence of the two-step procedure has been determined here using the following criteria:

- Initial localization: first, PM localization, until the gradient norm of the localization measure[79,23] is $G \leq 10^{-3}$, followed by ER localization: convergence of $\boldsymbol{\kappa} \approx \mathbf{0}$ determined by $\kappa_{\mathrm{max}} \leq 10^{-1}$, $\kappa_{\mathrm{rms}} \leq 10^{-1}$, and change in self-repulsion energy in the last step $|\delta E| \leq 1$.
- Unitary optimization: convergence of $\boldsymbol{\kappa} \approx \mathbf{0}$ determined by $\kappa_{\mathrm{max}} \leq 10^{-3}$, $\kappa_{\mathrm{rms}} \leq 10^{-4}$, and change in SI energy in the last step $|\delta E| \leq 10^{-5}$.
- SCF convergence: change in density from the last SCF step $\Delta P_{\mathrm{max}}^{\sigma} \leq 10^{-7}$, $\Delta P_{\mathrm{rms}}^{\sigma} \leq 10^{-8}$ and change in energy $|\Delta E| \leq 10^{-8}$.
- Convergence of self-consistent procedure: change in density from the last cycle $\Delta P_{\mathrm{max}}^{\sigma} \leq 10^{-5}$, $\Delta P_{\mathrm{rms}}^{\sigma} \leq 10^{-6}$, and change in energy $|\Delta E| \leq 10^{-5}$.

Here, the maximum and root-mean-square measures are defined by

dx.doi.org/10.1021/ct500637x | J. Chem. Theory Comput. XXXX, XXX, XXX–XXX

$$\Delta P^{\sigma}_{\max} := \max_{\mu\nu} |\Delta P^{\sigma}_{\mu\nu}| \tag{51}$$

$$\Delta P^{\sigma}_{\mathrm{rms}} := \sqrt{\frac{1}{K^2} \sum_{\mu\nu=1}^{K} (\Delta P^{\sigma}_{\mu\nu})^2} \tag{52}$$

where the density change matrix is

$$\Delta \mathbf{P}^{\sigma} = \mathbf{P}^{\sigma}_{\mathrm{new}} - \mathbf{P}^{\sigma}_{\mathrm{old}} \tag{53}$$

A tight unitary optimization is not worthwhile in the initial cycles of the procedure, since the underlying density may change radically upon the introduction of the SIC. For this reason, we have limited the amount of steps to be taken in the unitary optimization to a maximum of 10. To determine whether the SI energy has changed upon refinement of the CMOs, at least one step is taken in the unitary optimization.

RESULTS

Convergence and Sensitivity to Starting Point. An electronic structure algorithm should reliably converge on the global minimum. Unfortunately, as was discussed in the Theory section, in addition to the possibility of convergence to a higher local minimum, most SCF convergence accelerator algorithms may also converge onto a saddle point (SP). SP convergence should not be a problem in the unitary optimization for two reasons. First, the conjugate gradient method used in the unitary optimization does not have a tendency to converge to SPs. Second, the unitary optimization is only part of the procedure; it is followed by the solution of a new SCF density in the effective field generated by the unitary optimized orbitals. In case the unitary optimization converges onto a SP, the density update is likely to move the algorithm off the SP. The next unitary optimization should then find a proper local minimum. However, as was discussed in the Introduction, in extended systems, the PZ-SIC scheme may allow both localized and delocal solutions, which implies that the PZ-SIC functional may have multiple local minima.

The sensitivity of the algorithm to the starting point was tested with calculations on the acrylic acid and benzene molecules. Unless otherwise stated, the calculations in the present manuscript have been performed using the aug-cc-pCVTZ basis set.[113−115] The molecular geometries have been optimized with all-electron Møller−Plesset perturbation theory[116] truncated at the second order, using the CFOUR program.[117] The sampling was done by starting the unitary optimization procedure from a set of random matrices. The results for complex OMOs, given in Table 1, show that the procedure performs satisfactorily. For benzene, the largest difference in the energies reproduced by the 10 calculations is just twice the convergence threshold that is used. Because the convergence of the self-consistent procedure is determined by the change in the energy in the *last macroiteration*, an error of this magnitude is certainly acceptable.

For acrylic acid, the situation is somewhat different. Here, five calculations reproduce the same final energy with a similar accuracy as seen for benzene, but the other five give varying energies that are $3-6 \times 10^{-3}$ millihartrees above the value given by the former calculations. We believe that this difference in the behavior of the algorithm is due to the different chemical structure of the two molecules. Benzene is a symmetric molecule, with only two types of bonds, and thus has little variational freedom to divide the total electron density into the OMOs while maintaining the symmetry. Acrylic acid, on the other hand, has more types of bonds and a lower symmetry, both of which make the optimization problem harder. Here, convergence has clearly occurred to either a saddle point or another local minimum.

Table 1. Final Energy of Benzene and Acrylic Acid, Sampled from 10 Different Random Starting Points for the Unitary Optimization[a]

	Energy	
starting point	benzene	acrylic acid
1	−232.12437	−267.04257
2	−232.12436	−267.03940
3	−232.12435	−267.04255
4	−232.12435	−267.03914
5	−232.12436	−267.03882
6	−232.12435	−267.04257
7	−232.12436	−267.04255
8	−232.12436	−267.03957
9	−232.12437	−267.04258
10	−232.12437	−267.03676

[a]Complex OMOs were used.

The results with real OMOs were found to be similar to those for complex OMOs presented above. The choice of the Hamiltonian (eqs 37 and 38) was not found to affect the convergence characteristics of the algorithm.

Energy of Atoms. The energy of atoms ranging from H to Ar was calculated using various functionals (see Figure 2). Analogous calculations for an LDA xc functional and the Perdew−Burke−Ernzerhof (PBE) xc functional[102,103] have been presented previously.[68] The error in the calculations is estimated by comparison with accurate *ab initio* estimates from refs 104 and 105. Results are shown for three different GGA exchange functionals: APBE,[106] PBEsol,[107] and PBE. For consistency, all three exchange functionals were combined with the PBE correlation functional.[102] For PBEsol exchange, results with PBEsol correlation also are shown.[107] The figure presents results obtained with the TPSS functional, which has a mGGA form,[108,109] as well.

Results for both real and complex orbitals are shown. In general, the difference between real and complex orbitals is only seen for $Z \geq 5$. Up to $Z = 4$, only two orbitals exist per spin channel, and the complex degree of freedom adds no more flexibility to the orbital density, as all transforms can be spanned with a single parameter. At least three orbitals per channel are necessary to require the additional freedom introduced by the complex unitary transform.

As has been pointed out previously, it is necessary to use complex OMOs for PZ-SIC. The importance of using complex OMOs is particularly evident from the results using the TPSS mGGA functional. While the energy per electron in the atoms is quite well-reproduced by TPSS, the PZ-SIC leads to large errors when the OMOs are restricted to real functions. However, these errors do not occur when the OMOs are complex functions, and the PZ-SIC then even provides a slight improvement over the TPSS results obtained in KS-DFT.

While PBEsol exchange is much worse in reproducing the atomic energies in KS-DFT—as can be expected, since it was fitted to reproduce properties of solids—when combined with the PZ-SIC procedure, it even surpasses the performance of the PBE and APBE exchange functionals. Interestingly, PBEsol exchange works better with PBE correlation than with PBEsol

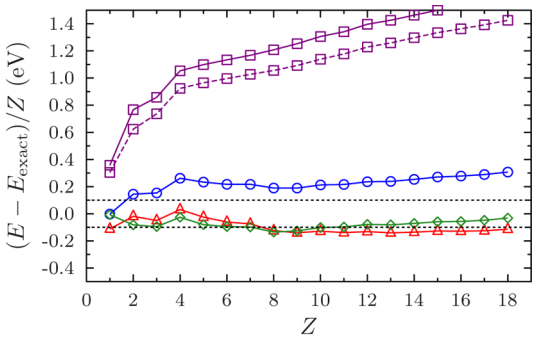

(a) Conventional KS-DFT.

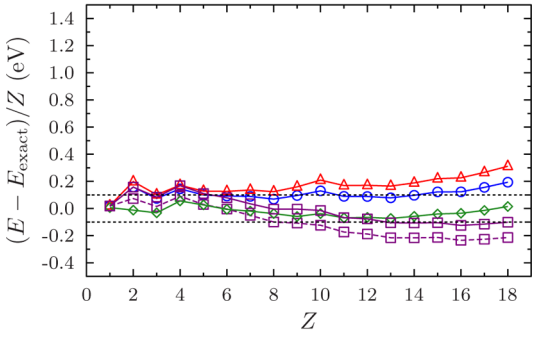

(b) PZ-SIC with real orbitals.

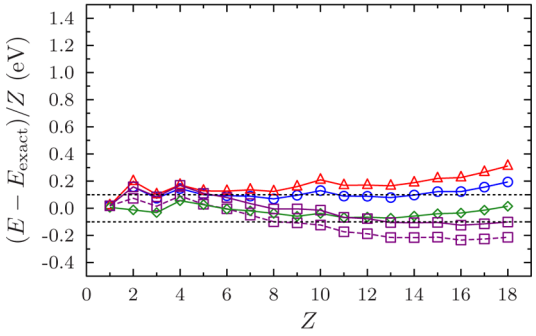

(c) PZ-SIC with complex orbitals.

Figure 2. Effect of PZ-SIC on energy of atoms. Legend: PBE exchange (solid blue line with circles), APBE exchange (solid red line with triangles), and PBEsol exchange (solid magenta line with squares), all of which were combined with the PBE correlation functional; and TPSS exchange-correlation (green diamonds). Shown are also results for PBEsol exchange combined with PBEsol correlation (dashed magenta line with squares). All the calculations were performed using the cc-pVQZ basis set.

correlation under the PZ-SIC, while the reverse is true for KS-DFT.

The gradient-dependent exchange enhancement factor in the PBEsol functional is weaker than for PBE, i.e., the exchange is closer to LDA. These results indicate that a strong gradient-dependent exchange enhancement factor is not needed when PZ-SIC is applied. Interestingly, while the three PBE-style exchange functionals used here give widely different results for the energy of the atoms in KS-DFT, the PZ-SIC greatly reduces the difference. In other words, the PZ-SIC reduces the dependence on the functional used. However, a new, optimal exchange enhancement factor should ideally be developed for the PZ-SIC form of the functional.[68,69]

Although one might expect the basis set requirements to change drastically by the introduction of the orbital-dependent SI energy, we found the basis set convergence of the atomic SIC energies to be similar to that of conventional KS-DFT, the cc-pVQZ basis already yielding convergence to the values displayed in Figure 2. The convergence of the PZ-SIC energy was also checked with the homoatomic dimers N_2 and O_2 at the LDA,[6,110,111] PBE,[102] and TPSS[108,109] levels of theory. Experimental bond lengths[112] of 1.098 Å and 1.208 Å, respectively, were used for the nitrogen and oxygen dimers. Again, the basis set convergence at the PZ-SIC level of theory was found to be similar to that at the KS-DFT level of theory.

Convergence. The convergence of the self-consistent PZ-SIC process is illustrated in Figure 3 for a PBE calculation on

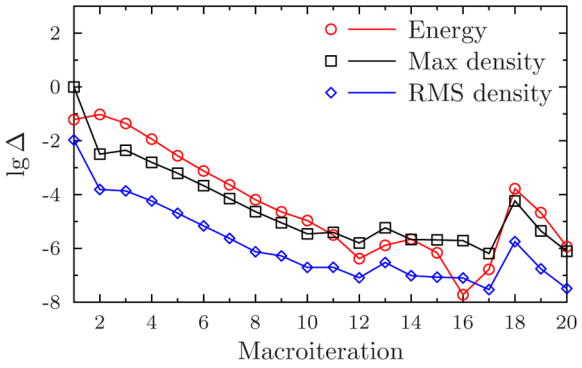

(a) Convergence of energy and density matrix.

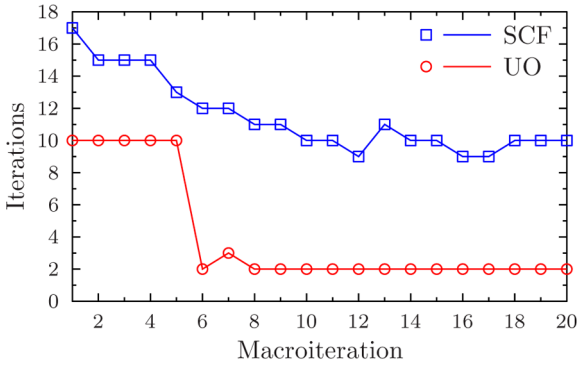

(b) Number of steps taken in the unitary optimization (UO) and the SCF calculation.

Figure 3. Convergence of self-consistent PZ-SIC calculations for benzene: (a) Convergence of energy and density matrix and (b) number of steps taken in the unitary optimization (UO) and the SCF calculation. In the first macroiteration, 10 microiterations are taken in the unitary optimization. The line search in every microiteration takes 4 evaluations, each of which requires the formation of 21 orbital self-interaction Fock matrices, totalling 840 Fock matrix builds in the unitary optimization of the first macroiteration. In comparison, the SCF solution in the first macroiteration only requires 17 iterations, each of which entailing a single Fock matrix build.

benzene C_6H_6. The bump visible in the last iterations of Figure 3a is caused by the switching to a more-accurate xc integration grid after self-consistency has been achieved with the initial accuracy grid.

The PBE-SIC calculation was initialized with the converged PBE density. In the first macroiteration, the total energy increased from the PBE value by 61 millihartree, which is an

dx.doi.org/10.1021/ct500637x | J. Chem. Theory Comput. XXXX, XXX, XXX−XXX

order of magnitude smaller than the estimated self-interaction energy (−0.7677 Ha), implying a significant shift of density to the virtual orbitals. The successive macroiterations all resulted in a monotonic decrease in the energy, with the converged PBE-SIC energy of −232.1243 Ha (containing 0.1113 Ha of SI energy) being considerably less than the PBE energy (−232.0241 Ha).

Optimal Orbitals. Although the orbital dependence of the energy obtained from PZ-SIC functionals, i.e., the lack of unitary invariance, represents a significant additional complexity in the variational calculations, it also results in more-informative results. While KS functional calculations typically give delocal CMOs, which are arbitrary in that any rotation of the orbitals gives the same total energy, and such calculations are often followed by some type of post-processing to determine more meaningful localized orbitals, calculations using PZ-SIC functionals give specific, optimal orbitals, which is consistent with the estimate of the energy. The complex OMOs obtained from PZ-SIC applied to the PBE functional for Ne and N_2 have been discussed previously[68,69] and similar results have been obtained from the present implementation.

Figure 4 shows OMOs obtained for a more-complex molecule (acrylic acid), using the PBE functional and

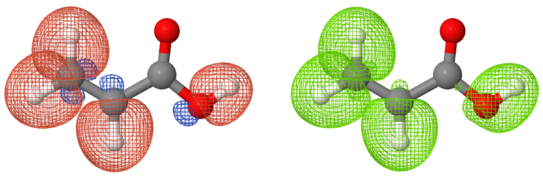

(a) CH and OH bonds. Left: real orbitals, right: complex orbitals.

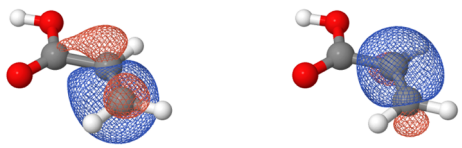

(b) CC double bond, real orbitals.

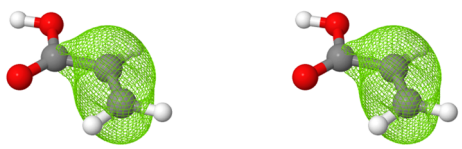

(c) CC double bond, complex orbitals.

Figure 4. Optimal molecular orbitals of an acrylic acid molecule obtained from a variational, self-consistent PZ-SIC calculation using the PBE functional: (a) CH and OH bonds ((left) real orbitals and (right) complex orbitals); (b) CC double bond, real orbitals; and (c) CC double bond, complex orbitals. The details of the rendering process are given in the Appendix.

variational, self-consistent PZ-SIC. The orbitals are quite similar to those obtained using PM and ER localization post-processing of KS-DFT orbitals.[23,100] However, there is a drastic difference here between calculations using real and complex orbitals, similar to what has been noted previously for other molecules.[69] Again, it is seen that the complex OMOs have more hybridization of s and p orbitals.

Charge Localization. To study charge localization, which is a well-known problem in KS-DFT, calculations on the CH_3 + F^- complex were carried out for a set of xc functionals as well as at the Hartree−Fock (HF) level of theory. A planar geometry was used for CH_3. The resulting Mulliken charges and energy differences relative to gas-phase CH_3 and F^- are shown in Figure 5. For reference, results at the coupled cluster[118] level of theory with full single and double excitations and perturbative triple excitations[119−121] (CCSD(T)) were obtained with CFOUR.[117]

KS-DFT calculations have problems localizing the extra electron, leading to spurious fractional charges on the fragments. This is particularly clear for pure DFT functionals, which predict $CH_3^{-0.2}$ + $F^{-0.8}$ when the CF distance is 4.5 Å, approaching the limit of noninteracting fragments. Here, the apparently good performance of the hybrid PBE0 functional (containing 25% exact exchange) is misleading, as the charge on F does not converge to −1, but rather starts to increase again as the distance between the fragments is increased further.

In contrast, the PZ-SIC calculations are in remarkably good agreement with the CCSD(T) calculations. Both the partial charge and energy curves are similar in form, with PZ-SIC clearly outperforming the HF calculation.

SUMMARY AND DISCUSSION

We have described an algorithm for the implementation of variational, self-consistent Perdew−Zunger self-interaction correction (PZ-SIC) calculations for finite systems and atomic basis sets using complex optimal orbitals. We have proposed an approximation where the CMOs are real functions, as this greatly simplifies the implementation of the PZ-SIC procedure in pre-existing Kohn−Sham density functional theory (KS-DFT) programs. The algorithm has been implemented in the freely available ERKALE program,[92,93] and it was applied to calculations of the energy of atoms, molecular orbitals and charge localization. We have successfully reproduced earlier results on atoms with complex OMOs and expanded those to more functionals, including the TPSS functional of meta-GGA form.

The application to the CH_3 + F^- complex shows that PZ-SIC can provide similar accuracy to coupled-cluster methods. It has been suggested in previous work[68,69] that new, optimized exchange-correlation (xc) functionals of GGA and/or mGGA form should ideally be developed for PZ-SIC calculations. Our results on the energy of atoms support this conclusion, as slight modifications of the PBE exchange functional, reducing the exchange enhancement factor and thereby bringing the functional closer to LDA, were found to result in significant improvements in the accuracy.

The large computational effort involved in high-accuracy post-Hartree−Fock (post-HF) methods limits their applicability to small systems. In contrast, the PZ-SIC methodology is computationally simple and can be readily implemented by extending a KS-DFT program. The method is especially attractive because of its favorable scaling properties, applicability to the solid state and cost-efficient implementation in plane-wave or real space grid codes.[122] Although presented here only within the scope of atom-centered basis sets, the present algorithm also can be applied in calculations using plane waves or real-space grids to represent the orbitals. The computational cost of traditional KS-DFT calculations is dominated by the diagonalization step with computational effort scaling as $O(K^3)$. For plane wave or grid-based approaches, iterative diagonalization schemes are used instead, for which the scaling is $O(N^\sigma K^2)$, where $K \gg N^\sigma$. PZ-SIC does not modify the diagonalization step, but introduces a new step where the unitary trans-

dx.doi.org/10.1021/ct500637x | J. Chem. Theory Comput. XXXX, XXX, XXX−XXX

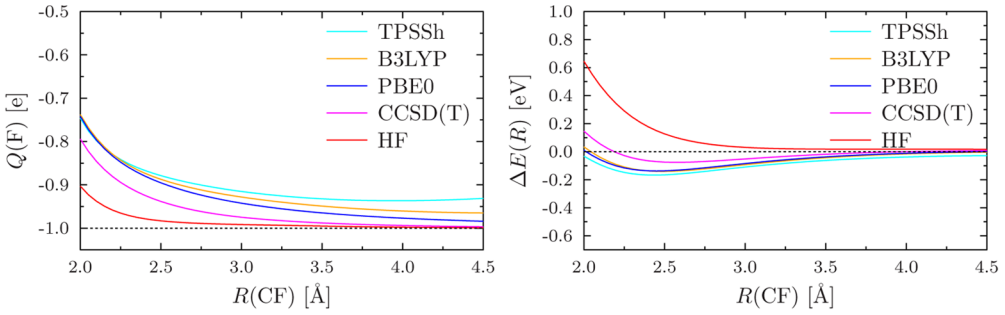

(a) Wave function methods and hybrid functionals.

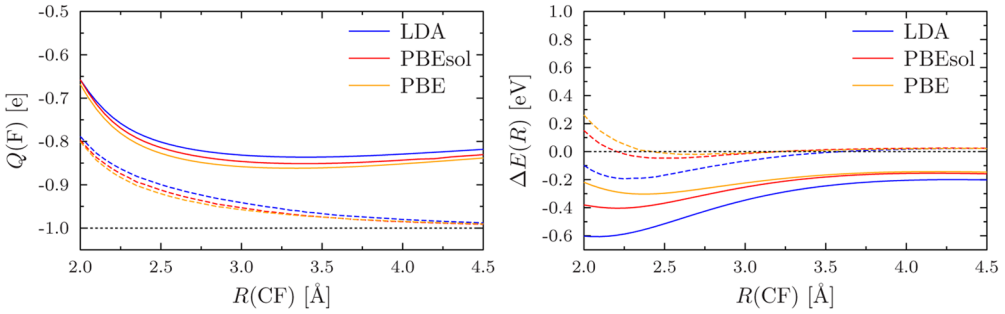

(b) Pure functionals. Solid lines denote conventional KS-DFT calculations, while dashed lines denote PZ-SIC calculations with complex orbitals.

Figure 5. Mulliken charge on the F atom and energy, each as a function of the CF distance in the $CH_3 + F^-$ complex. The charge on the F^- ion given by KS-DFT (both GGA and hybrid functionals) is fractional, while HF, CCSD(T), and PZ-SIC calculations applied to LDA, PBE, and PBEsol functionals properly give a charge of −1.

formation is optimized. At every step of the optimization for spin σ, the N^σ orbital xc potentials must be computed. (For a Coulomb-only treatment or the implementation of Hartree theory in Gaussian basis sets, a single set of integrals is enough to evaluate the interactions.) These tasks are independent and can easily be parallellized.

The computational cost of optimizing the $N^\sigma \times N^\sigma$ localizing matrices $\mathbf{W}^\sigma$ scales in principle as $O((N^\sigma)^2)$, resulting in a total scaling of $O((N^\sigma)^3)$ of the PZ-SIC procedure. Alternatively, as has been recently pointed out by Pederson et al.,[123] the $N^\sigma \times N^\sigma$ unitary optimization can be replaced by the optimization of the $3N^\sigma$ defining points of Fermi orbitals. While this would result in a remarkable decrease in the number of degrees of freedom ($3N^\sigma \ll (N^\sigma)^2$), the optimization of the Fermi orbital parameters is not as simple as the unitary optimization for which analytic gradients are easily available. Also, as is revealed by the argument for Fermi orbitals, the unitary optimization may converge faster than $O((N^\sigma)^2)$, because, in principle, only $3N^\sigma$ independent degrees of freedom are present in effect.

In practice, the unitary optimization dominates the computational cost of a PZ-SIC calculation because of its large prefactor. Computing the xc contribution is often the dominant cost in a KS-DFT calculation on small systems. In a PZ-SIC calculation, this cost is multiplied by the cost of computing a single point in the unitary optimization (the number of orbitals, typically on the order 10^2−10^3), and the number of points necessary to reach the optimum (another factor of 10^2). Thus, a prefactor of 10^4 is not unusual. But, real computational time—that is, wall clock time—increases much less since parallelization can easily be applied if enough processors are available. The embarrassingly parallel nature of the present algorithm is especially appealing for massively parallel supercomputers.

In the present work, the focus has been on the formulation of an efficient method to perform calculations within the variational, self-consistent PZ-SIC formalism. The method can be optimized further in many ways, but this is left for future work. One possibility is to screen out the better converged orbitals in the unitary optimization, focusing only on the orbitals for which κ_{ij} is large. Another possibility is to use effective core potentials or the projector augmented wave (PAW) method to describe the chemically inactive inner electrons. This is expected to maintain the accuracy of the method, while greatly reducing the computational effort. However, since PZ-SIC may result in significant changes to the core orbitals, new effective core potentials or PAW projectors must be developed for PZ-SIC. For instance, the eigenvalue of the lowest-lying canonical orbital in H_2O is −18.739 Hartree at the PBE/cc-pVTZ level of theory. The same calculation with PZ-SIC gives −20.534 Hartree, although the largest orbital SI energy in the calculation is only 0.0408 Hartree, with the other orbitals having *negative* SI energies, yielding a total SI energy of 0.0016 Hartree. The PZ-SIC eigenvalue is close to that reproduced by HF, which is −20.555 Hartree. (These numbers have been obtained with the symmetrized Hamiltonian of eq 37; the 1s energy is only slightly affected by the use of a unified Hamiltonian in eq 38.) The larger effect of the SIC on the orbital energies, compared to the total energy, is well-known.[13]

Some starting point sensitivity has been detected in the calculations of acrylic acid, which we have tentatively attributed to the possibility of multiple local minima in the PZ-SIC functional. However, SI effects are dominated by the exchange term; the correlation contribution is much smaller and is not as strongly dependent on molecular geometry.[124,125] Since most of the numerical problems associated with the present approach

dx.doi.org/10.1021/ct500637x | J. Chem. Theory Comput. XXXX, XXX, XXX−XXX

are likely related to handling the imperfect cancellation of the exchange and Coulomb interactions, another starting point for a SI free theory might prove more fruitful.

A different self-interaction correction procedure has been proposed by Lundin and Eriksson[40] (LU), where the electron density is corrected rather than the potentials. Although it is not evident that this scheme would leave the exact functional invariant, as PZ-SIC does, it might be more appropriate for approximate functionals. While the LU scheme is still non-unitary invariant, it may converge faster than PZ, because the density is smoother than the potential that can be singular and contain nodal surfaces. Again, further development of the LU approach and the adaption of the algorithm presented here to that method could be an interesting avenue for future work.

It would also be interesting to see whether a reparametrized exchange functional for the self-interaction free Coulomb interaction (i.e., Hartree theory), and thereby a non-unitary invariant functional, could prove to be an easier way to develop a functional of higher accuracy than (m)GGA functionals in KS-DFT. Our initial results show that calculations within Hartree theory are easy to converge with the current procedure. In PZ-SIC, the competition between the self-xc and self-Coulomb terms in the correction can impede convergence. Also, only considering the Coulomb interaction in the unitary optimization avoids the main computational effort of the present approach, which is the numerical evaluation of the orbital xc matrices.

In contrast to PZ-SIC, we have not found complex OMOs to be important in the limited set of Hartree theory calculations performed so far. Studying the OMO densities by eigendecompositions

$$\mathbf{p}_i = \sum_j n_i^j \mathbf{d}_i^j (\mathbf{d}_i^j)^{\mathrm{T}} \tag{54}$$

where $\mathbf{d}_i^j$ is an eigenorbital with occupation n_i^j, it can be seen that while real OMOs only have a single dominant eigenorbital $\mathbf{d}_i^k$ with $n_i^k \approx 1$, complex OMOs are composed of two eigenorbitals $\mathbf{d}_i^k$ and $\mathbf{d}_i^{k'}$. Possibly, the need for the complex OMOs arises in the PZ-SIC procedure due to the competition between the exchange and Coulomb contributions to the SI energy.

APPENDIX

For the visualization, the orbitals were computed with ERKALE on a grid with a spacing of 0.1 Å and then rendered with Jmol[126] with an isosurface value c, corresponding to an 85% cumulative density cutoff.[23,100] Positive isosurfaces are shown in blue, and negative ones are shown in red. For the complex case, the absolute value of the orbital is plotted in green.

AUTHOR INFORMATION

Corresponding Author

*E-mail: susi.lehtola@alumni.helsinki.fi.

Present Address

[¶]Chemical Sciences Division, Lawrence Berkeley National Laboratory, Berkeley, CA 94720, USA.

Notes

The authors declare no competing financial interest.

ACKNOWLEDGMENTS

S.L. gratefully acknowledges funding from the Magnus Ernrooth Foundation, and thanks David Stück for discussions. We thank CSC−IT Center for Science, Ltd. (Espoo, Finland) for providing computational resources for the present work. This work has been supported by the Academy of Finland through its Centers of Excellence (Grant No. 251748) and FiDiPro programs (Grant No. 263294).

REFERENCES

(1) Hohenberg, P.; Kohn, W. *Phys. Rev.* **1964**, *136*, B864.
(2) Kohn, W.; Sham, L. J. *Phys. Rev.* **1965**, *140*, A1133.
(3) Becke, A. D. *J. Chem. Phys.* **2014**, *140*, 18A301.
(4) Burke, K. *J. Chem. Phys.* **2012**, *136*, 150901.
(5) Perdew, J. P.; Ruzsinszky, A.; Tao, J.; Staroverov, V. N.; Scuseria, G. E.; Csonka, G. I. *J. Chem. Phys.* **2005**, *123*, 62201.
(6) Dirac, P. A. M. *Math. Proc. Cambridge Philos. Soc.* **1930**, *26*, 376.
(7) Perdew, J. P.; Jackson, K. A.; Pederson, M. R.; Singh, D. J.; Fiolhais, C. *Phys. Rev. B* **1992**, *46*, 6671.
(8) Becke, A. D. *J. Chem. Phys.* **1993**, *98*, 5648.
(9) Becke, A. D. *J. Chem. Phys.* **1993**, *98*, 1372.
(10) Cohen, A. J.; Mori-Sánchez, P.; Yang, W. *Science* **2008**, *321*, 792.
(11) Patchkovskii, S.; Ziegler, T. *J. Chem. Phys.* **2002**, *116*, 7806.
(12) Vydrov, O. A.; Scuseria, G. E. *J. Chem. Phys.* **2004**, *121*, 8187.
(13) Perdew, J. P.; Zunger, A. *Phys. Rev. B* **1981**, *23*, 5048.
(14) Foster, J.; Boys, S. *Rev. Mod. Phys.* **1960**, *32*, 300.
(15) Edmiston, C.; Ruedenberg, K. *Rev. Mod. Phys.* **1963**, *35*, 457.
(16) Norman, M. *Phys. Rev. B* **1983**, *28*, 3585.
(17) Pederson, M. R.; Heaton, R. A.; Harrison, J. G. *Phys. Rev. B* **1989**, *39*, 1581.
(18) Svane, A. *Phys. Rev. B* **1995**, *51*, 7924.
(19) Marzari, N.; Vanderbilt, D. *Phys. Rev. B* **1997**, *56*, 12847.
(20) Marzari, N.; Mostofi, A. A.; Yates, J. R.; Souza, I.; Vanderbilt, D. *Rev. Mod. Phys.* **2012**, *84*, 1419.
(21) Høyvik, I.-M.; Jansik, B.; Jørgensen, P. *J. Chem. Phys.* **2012**, *137*, 224114.
(22) Pipek, J.; Mezey, P. G. *J. Chem. Phys.* **1989**, *90*, 4916.
(23) Lehtola, S.; Jónsson, H. *J. Chem. Theory Comput.* **2014**, *10*, 642.
(24) von Niessen, W. *J. Chem. Phys.* **1972**, *56*, 4290.
(25) Hartree, D. R. *Math. Proc. Cambridge Philos. Soc.* **1928**, *24*, 89.
(26) Hartree, D. R. *Math. Proc. Cambridge Philos. Soc.* **1928**, *24*, 111.
(27) Hartree, D. R. *Math. Proc. Cambridge Philos. Soc.* **1928**, *24*, 426.
(28) Harrison, J. G.; Heaton, R. A.; Lin, C. C. *J. Phys. B: At. Mol. Phys.* **1983**, *16*, 2079.
(29) Goedecker, S.; Umrigar, C. J. *Phys. Rev. A* **1997**, *55*, 1765.
(30) Sharp, R.; Horton, G. *Phys. Rev.* **1953**, *90*, 317.
(31) Talman, J.; Shadwick, W. *Phys. Rev. A* **1976**, *14*, 36.
(32) Krieger, J. B.; Li, Y.; Iafrate, G. J. *Phys. Lett. A* **1990**, *148*, 470.
(33) Krieger, J. B.; Li, Y.; Iafrate, G. J. *Phys. Rev. A* **1992**, *45*, 101.
(34) Garza, J.; Nichols, J. A.; Dixon, D. A. *J. Chem. Phys.* **2000**, *112*, 7880.
(35) Perdew, J. P.; Parr, R. G.; Levy, M.; Balduz, J. L. *Phys. Rev. Lett.* **1982**, *49*, 1691.
(36) Li, Y.; Krieger, J. *Phys. Rev. A* **1990**, *41*, 1701.
(37) Gudmundsdóttir, H.; Zhang, Y.; Weber, P. M.; Jónsson, H. *J. Chem. Phys.* **2013**, *139*, 194102.
(38) Gudmundsdóttir, H.; Zhang, Y.; Weber, P. M.; Jónsson, H. *J. Chem. Phys.* **2014**, in press.
(39) Cheng, X.; Zhang, Y.; Deb, S.; Minitti, M. P.; Gao, Y.; Jónsson, H.; Weber, P. M. *Chem. Sci.* **2014**, *5*, 4394.
(40) Lundin, U.; Eriksson, O. *Int. J. Quantum Chem.* **2001**, *81*, 247.
(41) Novák, P.; Pickett, W. E.; Ku, W.; Wagner, F. R. *Phys. Rev. B* **2003**, *67*, 140403.
(42) Gräfenstein, J.; Kraka, E.; Cremer, D. *J. Chem. Phys.* **2004**, *120*, 524.
(43) Gräfenstein, J.; Kraka, E.; Cremer, D. *Phys. Chem. Chem. Phys.* **2004**, *6*, 1096.
(44) Garza, J.; Vargas, R.; Nichols, J. A.; Dixon, D. A. *J. Chem. Phys.* **2001**, *114*, 639.
(45) Patchkovskii, S.; Autschbach, J.; Ziegler, T. *J. Chem. Phys.* **2001**, *115*, 26.

(46) Patchkovskii, S.; Ziegler, T. *J. Phys. Chem. A* **2002**, *106*, 1088.
(47) Pemmaraju, C.; Archer, T.; Sánchez-Portal, D.; Sanvito, S. *Phys. Rev. B* **2007**, *75*, 045101.
(48) Vydrov, O. A.; Scuseria, G. E. *J. Chem. Phys.* **2005**, *122*, 184107.
(49) Harrison, J. G. *J. Chem. Phys.* **1983**, *78*, 4562.
(50) Harrison, J. G. *J. Chem. Phys.* **1983**, *79*, 2265.
(51) Harrison, J. G. *Chem. Phys. Lett.* **1983**, *96*, 181.
(52) Harrison, J. G. *J. Chem. Phys.* **1986**, *84*, 1659.
(53) Harrison, J. G. *J. Chem. Phys.* **1987**, *86*, 2849.
(54) Harrison, J. G. *Phys. Rev. B* **1987**, *35*, 987.
(55) Heaton, R. A.; Lin, C. C. *Phys. Rev. B* **1980**, *22*, 3629.
(56) Heaton, R. A.; Harrison, J. G.; Lin, C. C. *Solid State Commun.* **1982**, *41*, 827.
(57) Heaton, R. A.; Harrison, J. G.; Lin, C. C. *Phys. Rev. B* **1983**, *28*, 5992.
(58) Heaton, R. A.; Lin, C. C. *J. Phys. C Solid State Phys.* **1984**, *17*, 1853.
(59) Heaton, R. A.; Harrison, J. G.; Lin, C. C. *Phys. Rev. B* **1985**, *31*, 1077.
(60) Heaton, R. A.; Pederson, M. R.; Lin, C. C. *J. Chem. Phys.* **1987**, *86*, 258.
(61) Pederson, M. R.; Heaton, R. A.; Lin, C. C. *J. Chem. Phys.* **1984**, *80*, 1972.
(62) Pederson, M. R.; Heaton, R. A.; Lin, C. C. *J. Chem. Phys.* **1985**, *82*, 2688.
(63) Pederson, M. R.; Lin, C. C. *Phys. Rev. B* **1987**, *35*, 2273.
(64) Pederson, M. R.; Lin, C. C. *J. Chem. Phys.* **1988**, *88*, 1807.
(65) Pederson, M. R.; Klein, B. M. *Phys. Rev. B* **1988**, *37*, 10319.
(66) Vydrov, O. A.; Scuseria, G. E. *J. Chem. Phys.* **2006**, *124*, 191101.
(67) Vydrov, O. A.; Scuseria, G. E.; Perdew, J. P.; Ruzsinszky, A.; Csonka, G. I. *J. Chem. Phys.* **2006**, *124*, 94108.
(68) Klüpfel, S.; Klüpfel, P.; Jónsson, H. *Phys. Rev. A* **2011**, *84*, 050501.
(69) Klüpfel, S.; Klüpfel, P.; Jónsson, H. *J. Chem. Phys.* **2012**, *137*, 124102.
(70) Pederson, M. R.; Perdew, J. P. *Psi-K Newsl. Sci. Highlight Month* **2012**, 77 (URL: http://www.psi-k.org/newsletters/News_109/Highlight_109.pdf).
(71) Tsuneda, T.; Hirao, K. *J. Chem. Phys.* **2014**, *140*, 18A513.
(72) Roothaan, C. *Rev. Mod. Phys.* **1951**, *23*, 69.
(73) Pople, J. A.; Nesbet, R. K. *J. Chem. Phys.* **1954**, *22*, 571.
(74) Pople, J. A.; Gill, P. M. W.; Johnson, B. G. *Chem. Phys. Lett.* **1992**, *199*, 557.
(75) Helgaker, T.; Jørgensen, P.; Olsen, J. *Molecular Electronic-Structure Theory*; John Wiley & Sons, Ltd.: New York, 2000; p 438.
(76) Saunders, V. R.; Hillier, I. H. *Int. J. Quantum Chem.* **1973**, *7*, 699.
(77) Abrudan, T. E.; Eriksson, J.; Koivunen, V. *IEEE Trans. Signal Process.* **2008**, *56*, 1134.
(78) Abrudan, T.; Eriksson, J.; Koivunen, V. *Signal Process.* **2009**, *89*, 1704.
(79) Lehtola, S.; Jónsson, H. *J. Chem. Theory Comput.* **2013**, *9*, 5365.
(80) Messud, J.; Dinh, P.; Reinhard, P.-G.; Suraud, E. *Ann. Phys. (N.Y.)* **2009**, *324*, 955.
(81) Hofmann, D.; Klüpfel, S.; Klüpfel, P.; Kümmel, S. *Phys. Rev. A* **2012**, *85*, 062514.
(82) Ostlund, N. S. *J. Chem. Phys.* **1972**, *57*, 2994.
(83) Edwards, W. D. *Int. J. Quantum Chem.* **1988**, *34*, 549.
(84) Pulay, P. *Chem. Phys. Lett.* **1980**, *73*, 393.
(85) Pulay, P. *J. Comput. Chem.* **1982**, *3*, 556.
(86) Kudin, K. N.; Scuseria, G. E.; Cancès, E. *J. Chem. Phys.* **2002**, *116*, 8255.
(87) Van Voorhis, T.; Head-Gordon, M. *Mol. Phys.* **2002**, *100*, 1713.
(88) Thøgersen, L.; Olsen, J.; Yeager, D.; Jørgensen, P.; Sałek, P.; Helgaker, T. *J. Chem. Phys.* **2004**, *121*, 16.
(89) Hu, X.; Yang, W. *J. Chem. Phys.* **2010**, *132*, 054109.
(90) Seeger, R.; Pople, J. A. *J. Chem. Phys.* **1977**, *66*, 3045.
(91) Bauernschmitt, R.; Ahlrichs, R. *J. Chem. Phys.* **1996**, *104*, 9047.
(92) Lehtola, S. *ERKALE—HF/DFT from Hel*, 2013. Available via the Internet at http://erkale.googlecode.com.
(93) Lehtola, J.; Hakala, M.; Sakko, A.; Hämäläinen, K. *J. Comput. Chem.* **2012**, *33*, 1572.
(94) Marques, M. A. L.; et al., Libxc—A library of exchange-correlation functionals for density-functional theory. Available via the Internet at http://tddft.org/programs/octopus/wiki/index.php/Libxc.
(95) Marques, M. A. L.; Oliveira, M. J. T.; Burnus, T. *Comput. Phys. Commun.* **2012**, *183*, 2272.
(96) Baerends, E. J. *Chem. Phys.* **1973**, *2*, 41.
(97) Sambe, H.; Felton, R. H. *J. Chem. Phys.* **1975**, *62*, 1122.
(98) Yang, R.; Rendell, A. P.; Frisch, M. J. *J. Chem. Phys.* **2007**, *127*, 074102.
(99) Van Lenthe, J. H.; Zwaans, R.; Van Dam, H. J. J.; Guest, M. F. *J. Comput. Chem.* **2006**, *27*, 926.
(100) Knizia, G. *J. Chem. Theory Comput.* **2013**, *9*, 4834.
(101) Köster, A. M.; Flores-Moreno, R.; Reveles, J. U. *J. Chem. Phys.* **2004**, *121*, 681.
(102) Perdew, J. P.; Burke, K.; Ernzerhof, M. *Phys. Rev. Lett.* **1996**, *77*, 3865.
(103) Perdew, J. P.; Burke, K.; Ernzerhof, M. *Phys. Rev. Lett.* **1997**, *78*, 1396.
(104) Davidson, E.; Hagstrom, S.; Chakravorty, S.; Umar, V.; Fischer, C. *Phys. Rev. A* **1991**, *44*, 7071.
(105) Chakravorty, S. J.; Davidson, E. R. *J. Phys. Chem.* **1996**, *100*, 6167.
(106) Constantin, L. A.; Fabiano, E.; Laricchia, S.; Della Sala, F. *Phys. Rev. Lett.* **2011**, *106*, 186406.
(107) Perdew, J. P.; Ruzsinszky, A.; Csonka, G. I.; Vydrov, O. A.; Scuseria, G. E.; Constantin, L. A.; Zhou, X.; Burke, K. *Phys. Rev. Lett.* **2008**, *100*, 136406.
(108) Tao, J.; Perdew, J. P.; Staroverov, V. N.; Scuseria, G. E. *Phys. Rev. Lett.* **2003**, *91*, 146401.
(109) Perdew, J. P.; Tao, J.; Staroverov, V. N.; Scuseria, G. E. *J. Chem. Phys.* **2004**, *120*, 6898.
(110) Bloch, F. *Z. Phys.* **1929**, *57*, 545.
(111) Vosko, S. H.; Wilk, L.; Nusair, M. *Can. J. Phys.* **1980**, *58*, 1200.
(112) Huber, K. P.; Herzberg, G.; Gallagher, J. W.; R. D. Johnson, I. In *NIST Chemistry WebBook*; Linstrom, P. J., Mallard, W. G., Eds.; National Institute of Standards and Technology, Gaithersburg MD; NIST Standard Reference Database Number 69.
(113) Dunning, T. H. *J. Chem. Phys.* **1989**, *90*, 1007.
(114) Kendall, R. A.; Dunning, T. H.; Harrison, R. J. *J. Chem. Phys.* **1992**, *96*, 6796.
(115) Woon, D. E.; Dunning, T. H. *J. Chem. Phys.* **1995**, *103*, 4572.
(116) Møller, C.; Plesset, M. S. M. *Phys. Rev.* **1934**, *46*, 618.
(117) CFOUR, a quantum chemical program package, written by: (a) Stanton, J. F.; Gauss, J.; Harding, M. E.; Szalay, P. G., with contributions from (b) Auer, A. A.; Bartlett, R. J.; Benedikt, U.; Berger, C.; Bernholdt, D. E.; Bomble, Y. J.; Cheng, L.; Christiansen, O.; Heckert, M.; Heun, O.; Huber, C.; Jagau, T.-C.; Jonsson, D.; Jusélius, J., Klein, K.; Lauderdale, W. J.; Matthews, D. A.; Metzroth, T.; Mück, L. A., O'Neill, D. P., Price, D. R.; Prochnow, E.; Puzzarini, C.; Ruud, K.; Schiffmann, F.; Schwalbach, W.; Simmons, C.; Stopkowicz, S.; Tajti, A.; Vázquez, J.; Wang, F.; Watts, J. D. and the integral packages (c) MOLECULE (Almlöf, J.; Taylor, P. R.), (d) PROPS (Taylor, P. R.), (e) ABACUS (Helgaker, T.; Jensen, H. J. Aa., Jørgensen, P.; Olsen, J.), and (f) ECP routines by Mitin, A. V.; van Wüllen, C. For the current version, see http://www.cfour.de.
(118) Cížek, J. *J. Chem. Phys.* **1966**, *45*, 4256.
(119) Raghavachari, K.; Trucks, G. W.; Pople, J. A.; Head-Gordon, M. *Chem. Phys. Lett.* **1989**, *157*, 479.
(120) Bartlett, R. J.; Watts, J. D.; Kucharski, S. A.; Noga, J. *Chem. Phys. Lett.* **1990**, *165*, 513.
(121) Stanton, J. F. *Chem. Phys. Lett.* **1997**, *281*, 130.
(122) Valdés, A.; et al. *Phys. Chem. Chem. Phys.* **2012**, *14*, 49.
(123) Pederson, M. R.; Ruzsinszky, A.; Perdew, J. P. *J. Chem. Phys.* **2014**, *140*, 121103.
(124) Johnson, B. G.; Gonzales, C. A.; Gill, P. M.; Pople, J. A. *Chem. Phys. Lett.* **1994**, *221*, 100.
(125) Csonka, G. I.; Johnson, B. G. *Theor. Chem. Acc.* **1998**, *99*, 158.

(126) *Jmol: An open-source Java viewer for chemical structures in 3D*. Available via the Internet at http://www.jmol.org.